International Journal of Solids and Structures 50 (2013) 3089–3096

Contents lists available at SciVerse ScienceDirect

International Journal of Solids and Structures

journal homepage: www.elsevier.com/locate/ijsolstr

Large bending behavior of creased paperboard. I. Experimental investigations

Lando Mentrasti [a,*], Ferdinando Cannella [b], Mirko Pupilli [c], Jian S. Dai [d]

[a] Dipartimento di Ingegneria Civile, Edile e Architettura, Facoltà di Ingegneria, Università Politecnica delle Marche, Via Brecce Bianche, 60131 Ancona, Italy
[b] Department of Advanced Robotics, Italian Institute of Technology, Via Morego 30, 16163 Genova, Italy
[c] Dipartimento di Meccanica, Facoltà di Ingegneria, Università Politecnica delle Marche, Via Brecce Bianche, 60131 Ancona, Italy
[d] Department of Mechanical Engineering, King's College London, University of London, Strand, London WC2R 2LS, United Kingdom

ARTICLE INFO

Article history:
Available online 6 June 2013

Keywords:
Creased paperboard
Large bending behavior
Unstable constitutive equations
Carton erection
Reconfigurable real-time carton formation robot

ABSTRACT

The large bending behavior of a creased paperboard is studied in the range of rotation $\theta \in [0°, 180°]$ – new results, apparently not reported previously in literature – with the aim to point out some crucial aspect involved in an adaptive robotic manipulation of the industrial cartons.

The loading tests show a **great variability** of the mechanical behavior, depending dramatically on the crease indentation depth (also for the specimens obtained from the *same* carton): (a) when the damage induced during the crease formation is relatively small, the bending response is unusually complex: the moment **constitutive function**, $m_L(\theta)$, presents (up to) **two peaks** followed by **unstable branches**; (b) for greater indentation, the $m_L(\theta)$ is monotone.

In the unloading case the response $m_U(\theta)$ is always monotone and is practically independent of the formation conditions of the crease. These behaviors can be easily described analytically using (piecewise) third degree splines.

In a companion paper, the erection of a typical carton corner with unstable constitutive behavior is fully analyzed to detect the possible criticalities.

1. Introduction

The mechanical characterization of the creased paperboard (carton) has recently received great attention from both experimental and theoretical point on view, with the aim to increase the reliability of the (reconfigurable) robots, manipulating origami-type cartons in packaging industry (Dai and Rees Jones, 1999; Dubey and Dai, 2006; Yao and Dai, 2008; Cannella and Dai, 2009).

1.1. Alternative approaches

Several different and alternative research directions can be devised to control the evolution of the folding process of a complex origami carton.

The **predictive modeling**: the crease formation is analyzed and simulated as a structure, with the purpose to predict the macroscopic mechanical behavior of the creased paperboard during folding (Carlsson et al., 1983 – an early particular simple delamination model in very small rotation – Barbier et al. 2005; Beex and Peerlings, 2009; Giampieri et al., 2011), *assuming* that the geometry, the constitutive equations of each component, the technological process and the environmental conditions *are know* a priori (Ostoja-Starzewski and Stahl, 2000; Ramasubramanian and Wang, 2007; Sato et al., 2008; Suhling et al., 1985; Vannucci, 2010).

The **carton simulation**: the carton erection process is analyzed to detect possible criticalities such as instabilities, vibrations, contacts, face interferences (Mullineux and Matthews, 2010), configuration singularities (Cannella et al., 2012), *assuming* that the macroscopic mechanical behavior of the crease *is known* a priori (Nygårds et al., 2009).

The **reconfigurable** carton formation **robot**: the analysis of a reconfigurable robot for the carton manufacturing is considered, with *real-time detection and control* of both carton faces placement and actuation forces.

The above considerations suggest to consider the predictive model to be not sufficiently reliable, owing to the non-controllability of the variables influencing the mechanical response, with particular attention on the crease parameters and the environmental conditions (the crease depth and moisture content, primarily). What is more, the most influencing quantities can be variable not only with time from a sample to the other, but is different for the creases belonging to the same carton, as result from the following tests (similar issues are addressed by Hicks et al., 2004).

* Corresponding author. Tel.: +39 071 2204567; fax: +39 071 220 4576.
E-mail addresses: mentrasti@univpm.it (L. Mentrasti), ferdinando.cannella@iit.it (F. Cannella), mpupilli@tiscali.it (M. Pupilli), jian.dai@kcl.ac.uk (J.S. Dai).

0020-7683/$ - see front matter © 2013 Elsevier Ltd. All rights reserved.
http://dx.doi.org/10.1016/j.ijsolstr.2013.05.018

Nomenclature

c, **n**, **d**	denote the crease typology: cut, normal, dashed, respectively	**T**, **B**, **L**, **R**	denote the top, bottom, left and right side of a carton, respectively
$m(\theta, \dot{\theta})$	moment per unit length of the crease [N mm/mm]	θ	crease rotation
$m_L(\theta)$	loading constitutive equation, $\dot{\theta} > 0$	$\dot{\theta}$	derivative of the rotation with respect to the time
$m_U(\theta)$	unloading constitutive equation, $\dot{\theta} < 0$	:=	Ratischauser's symbol of definition

In the recent years, the last approach is adopted and several projects have been carried out (Dubey and Dai, 2006; Yao and Dai, 2008; Cannella and Dai, 2009) towards the implementation of a reconfigurable real-time controlled robot being able to adapt the manufacturing process to the carton in production. Nonetheless, the simulation stage requires, among other factors, the consideration of the functional form of the constitutive law $m(\theta)$.

1.2. Experimental investigation

The pioneering experimental study by Nagasawa et al. (2003) presented the influence of the crease depth indentation on the response $m(\theta)$ of a creased paperboard, m being the moment per unit length of the crease and θ the folding angle, restricted in the range $[0°, 90°]$.

This work discusses the constitutive equation $m(\theta)$ of the different types of crease present in industrial cartons employed in food packaging. The response is obtained for a bending rotation varying from 0 to 180°, results not previously published, to the best knowledge of the authors. Furthermore, the unloading process is also registered – a phenomenon involved in the aperture of a pre-folded carton.

The main outcome is the great dependence of $m(\theta)$ on the process of formation of the individual crease: it varies from a monotone trend with an always positive stiffness (when the indentation depth is great) to a function presenting many **unstable branches** (for small indentation depth). It is important to emphasize that this behavior, so qualitatively different, is coexistent on the set of specimens obtained from *nominally identical creases* of the same carton.

1.3. Theoretical structural analysis

The kinematic and structural analysis of the erection of a typical carton is presented in a companion paper (Mentrasti et al., 2013),

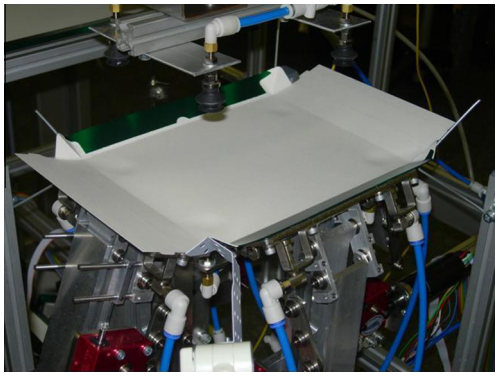

Fig. 2.1. An industrial carton (placed in the manipulator robot).

with the aim to show the possible criticalities due to the complex bending behavior. It is worth reaffirming here that a general procedure applicable to predict the structural behavior of an actual manufacturing carton is hardly reliable.

2. Experimental results

Several large rotation bending tests have been carried out on industrial carton employed in food packaging (Figs. 2.1 and 2.2(a)) with two average thickness: 0.40 mm, for two different cartons identified as *Th1* and *Th2*, and 0.44 mm for a carton identified as *Th3*.

The samples are obtained as follows:

- 3 or 4 samples are considered for each type of the crease as shown in Fig. 2.2:

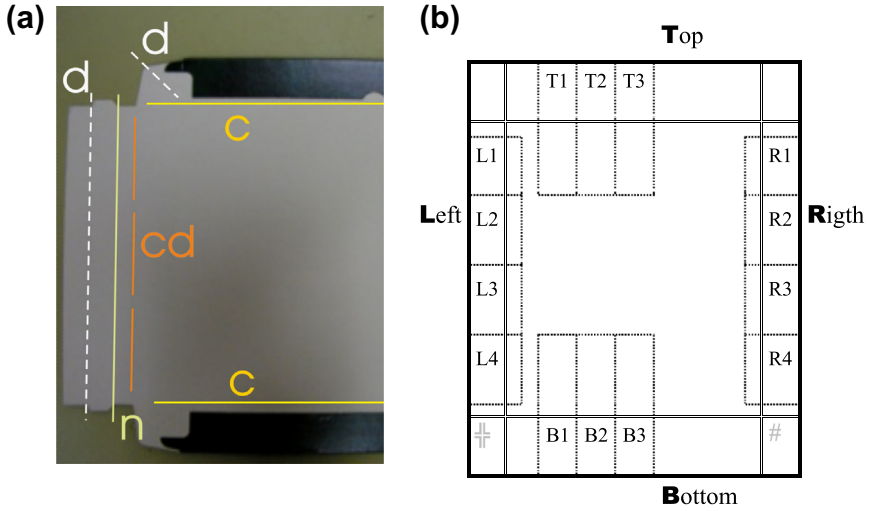

Fig. 2.2. (a) A typical carton (left side) with the crease types nomenclature; (b) Samples nomenclature within the a carton.

- (**n**) *normal* (standard) crease;
- (**c**) *continuous cut* crease (the cut traverses partially, but continuously, the paperboard thickness);
- (**d**) *dashed cut* crease (the cut traverses the paperboard thickness and is discontinuous). Creases *cut discontinuously* (**cd**) are not tested.

- a set of samples is obtained from the *different side of the same carton*: Left (**L**), Right (**R**), Top (**T**) and Bottom (**B**), according to Fig. 2.2;
- the bending is inward the crease, with rotation in the range 0–180°;
- each sample has been inflected in a monotone quasi-static loading (and unloading) in approximately 3 s, at 22–26 °C and 40–55% of relative humidity.
- the elastic bending of the very small portion of the paperboard adjacent to the crease is ignored.
- unloading has been immediately recorded without delay, after obtaining 180 degree rotation (cf. Allaoui et al., 2009).

The experimental setup is composed as follows: (1) the fix end of each sample is secured to a vertical plate support with a double side sticking tape; (2) the paperboard specimen is pushed at its free end by an L shaped aluminum beam, parallel to the crease; (3) it is supported by a load cell and rotates around the vertical axis of the rig, with an effective arm of 19.0 mm; (4) the rotation is detected by a high resolution encoder, coaxial with the crease. The load cell (Burster, Model 8511 EN, Bending Beam) has the following characteristics: 5.0 N Full Scale, 0.5% total accuracy (high linearity up to 0.1%) and maximum deflection of 0.15 mm (FS).

The moment per unit length $m(\theta)$ is finally computed taking into account the width of each specimen (between 45 and 50 mm). For each curve (load + unload) more than 1000 couple of values are detected.

It is perhaps appropriate to pointed out that the adopted testing methodology (the number of the samples per type of crease, the environmental condition, the conditioning of the samples, *etc.*) does not suggest either a new calibration or certification method, or an alternative protocol to identify the paperboard quality. More simply, our purpose is to draw attention to the never previously signaled facts presented below: the existence of multiple unstable branch in the bending response up to 180° and the unpredictability of the mechanical response of the creases of the same type belonging to the same carton (or of the "same" crease in different cartons of the same stock). Therefore, only a (statistically reasonable) minimum number of samples are considered. On the other hand, the actual dimensions the sides of the carton hardly permit a greater number of samples (3 for each short side, 4 for each long one, namely 6 or 8 samples per type of crease in each carton).

Besides, the tests are carried out under condition that can be considered very similar to a possible manufacturing environmental state. Several further results for different temperature and moisture conditions (stabilization of the cartons in a conditioned cell with humidity control; tests under heating conditions, with a real-time detection of the temperature; scattering analysis; *etc.*) are reported in "Mechanical Properties of Carton Creases" by Cannella et al., 2013.

In summary, a single cartoon (named **c00***X*_**Th***Y*, where *X* is the carton number and *Y* identifies the above mentioned thickness code) provide the samples identified as (*cf.* Fig. 2.2(b)):

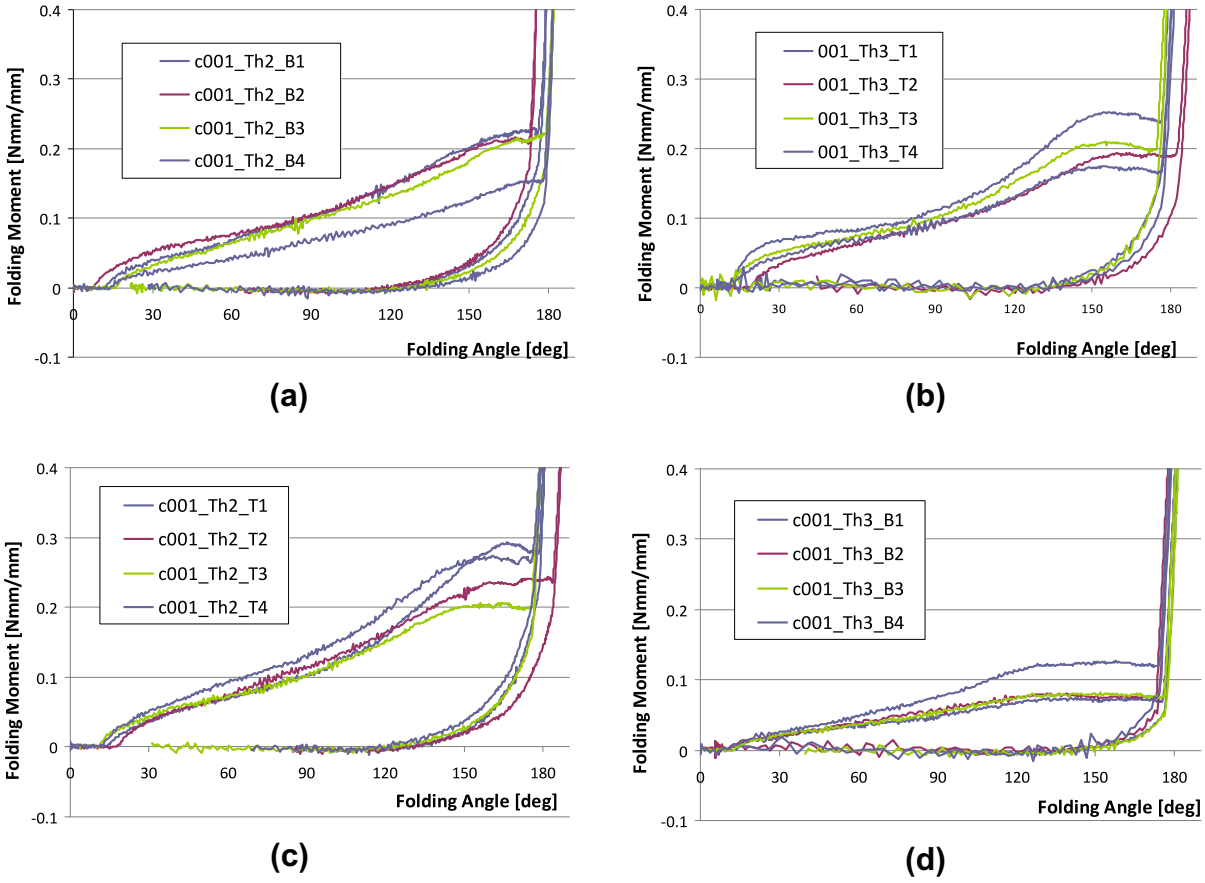

Fig. 2.3. Some typical diagram for the *cut creases* (**c**) located at the top (b,c) or bottom (a,d) position, in cartons of different thickness.

cT1, cT2, cT3, (continuous cut)
nL1, nL2, nL3, nR1, nR2, nR3, *(normal cut)*
dL1, dL2, dL3, dR1, dR2, dR3, *(dashed cut)*
cB1, cB2, cB3, *(continuous cut)*.

2.1. Experimental results for loading and unloading conditions

The paperboard sample is folded around the crease under quasi-static monotone *loading condition*, in the range $\theta \in [0, 180°]$ with $\dot{\theta} > 0$, $\dot{\theta}$ being the time derivative of the rotation; the obtained response is denoted $m_L(\theta)$. The *unloading condition* occurs when $\theta \in [\theta_U, 180°]$ with $\dot{\theta} < 0$; the response is denoted $m_U(\theta)$.

The results of the most significant assays are reported as coarse data without averaging or regularization, collected according to the crease type and the side of the carton. For some curve, the origin of the θ axis is slightly shifted for a better reading of the graph: however, the actual *end* of each loading diagram can be unambiguously identified by the vertical asymptote, necessarily located at 180°. On the other hand, the starting point is not well definite because often the moment becomes significant when $\theta > \sim$10–20°, owing to an initial natural curvature of the paperboard.

2.1.1. Continuous cut crease (**c**) results

This is the less significant response, due to the heavy damage caused by the continuous partial cut across the cross section of the paperboard: the diagram mL(θ) is practically linear in the whole range, with very low stiffness, independently of both the sides (**T** or **B**) and the carton sample tested (Fig. 2.3). Dispersion of the responses, also within the same side of the carton, is significant.

Unloading curve is coarsely parabolic without correlation with the loading curve, leading rapidly to $m = 0$ (in an interval of 30–60°).

2.1.2. Dashed cut crease (**d**) results

For this type of crease $m_L(\theta)$ attains highest values (Fig. 2.4). The curve can be compared to the elastic-perfectly plastic behavior of a traditional material, with relatively small dispersion (even if sides **L** and **R** can have different responses). It is very interesting to notice a modest, but well identifiable, *S-shaped* part of the diagram after the peak around 40–50°. It is a characteristic of the light indented normal creases (as widely discussed below) and, in the dashed creases, the moderate amount of the phenomenon can be attributed to the undamaged (not pre-indented!) integral part of paperboard between the cuts.

The unloading curves are roughly parabolic, but in this case the stiffness of m_U at $\theta = 180°$ is very close to the stiffness of m_L at the initial loading path. The value $m = 0$ is attained in 60–80°.

2.1.3. Normal crease (**n**) results

The standard *normal crease* (**n**), bent according to its indentation, shows the more interesting behavior, never observed in a structural materials of comparably simple composition. Our experimental investigation shows (Fig. 2.5):

- a second peak of m_L exists around 90°; it is usually markedly greater than the maximum detected by Nagasaawa et al. around 35°;
- a second more pronounced unstable branch follows this maximum;

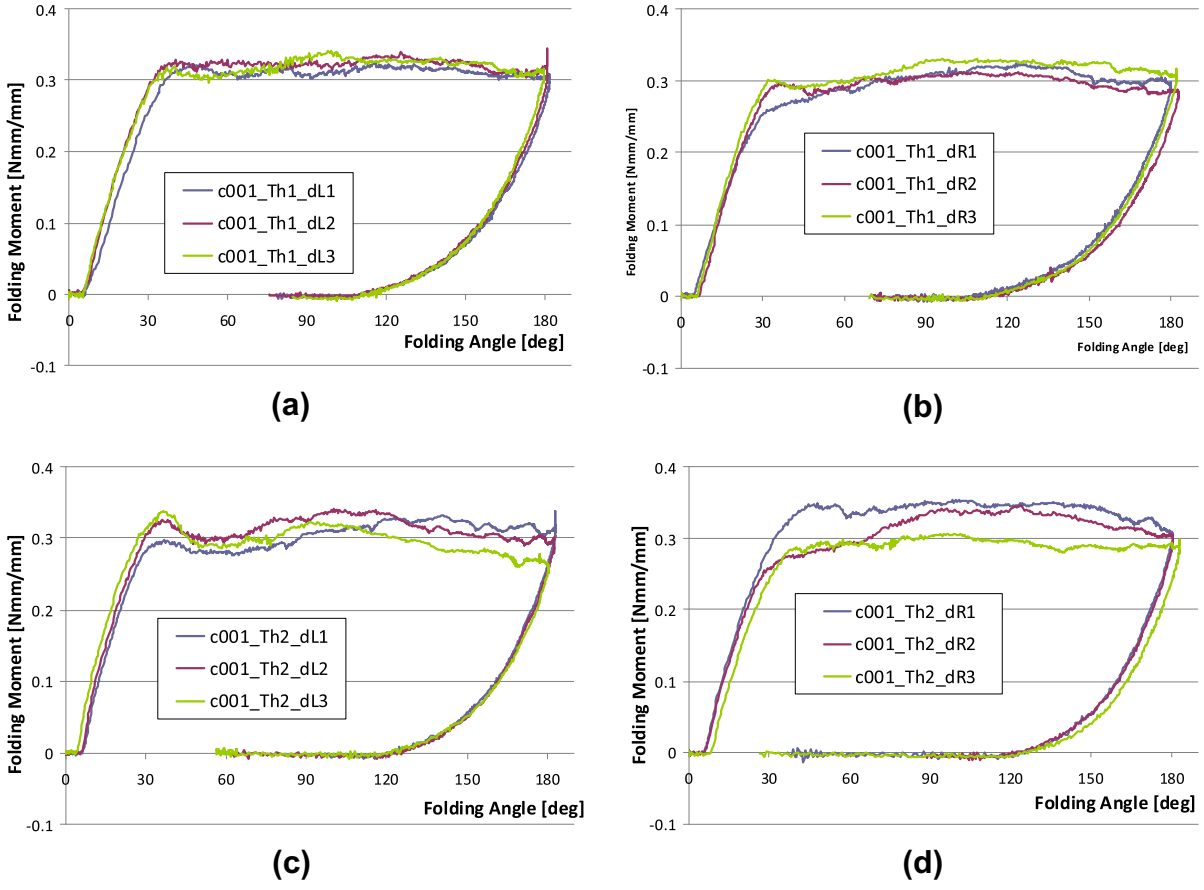

Fig. 2.4. Some typical diagram for the *dashed cut* creases (**d**).

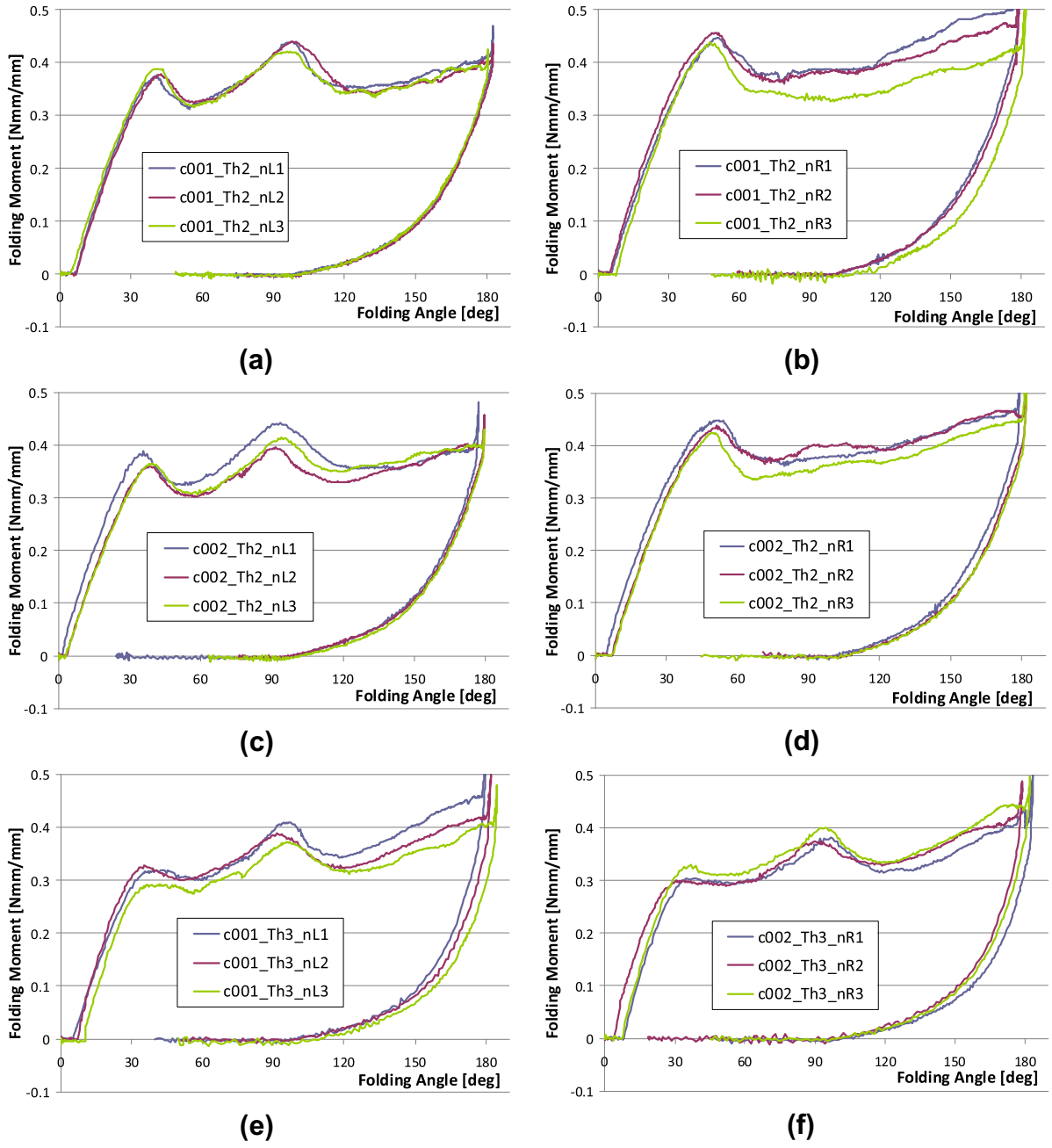

Fig. 2.5. Some typical diagram for the *normal* creases (**n**).

- the curve $m_L(\theta)$ is monotone increasing up to 180°, where an absolute maximum can be eventually attained.

In this circumstance the markedly different response of the **L** and **R** sides *of the same carton* is detected.

The unloading behavior is nearly parabolic with the unloading starting stiffness close to the initial loading stiffness, as in the previous case. The non-trivial unloading range has now a proportionally greater extent ($m = 0$, when $\theta \sim 90°$).

2.2. Peculiar crease-dependence of the bending behavior

A remarkable issue of the experimental tests, hitherto never pointed out, is the possible greatly dissimilar mechanical behavior of apparently identical crease (**n**) on different side or position in the same carton, as can be seen comparing the results shown in Figs. 2.6 and 2.5.

The explanation of this strange outcome is attributed to the different indentation during the crease formation. The conjecture is supported by the macrographs (30×) of *unbent* slices of paperboard obtained from the different side of the same carton. Fig. 2.7 clearly show the different crease depths (together with a consequently different damage).

Fig. 2.8 shows several micrographs: two unbent samples, obtained from the left and right side of the same carton, with small (a) and large (b) amount of delamination; (c) large indented sample after a bending of ∼45°. The standard histological preparation emphasizes the damaged layers in the different cases.

3. Bending constitutive equations

The experimental curves $m(\theta)$, obtained for the different crease types subject to one loading + unloading cycle, are idealized in four

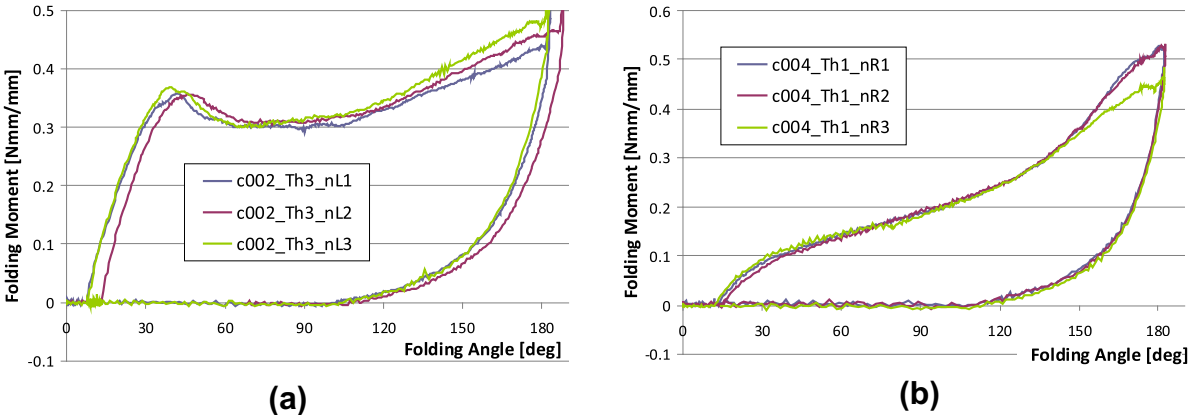

Fig. 2.6. Anomalous behavior of some *normal* creases (**n**) imputable to a large indentation.

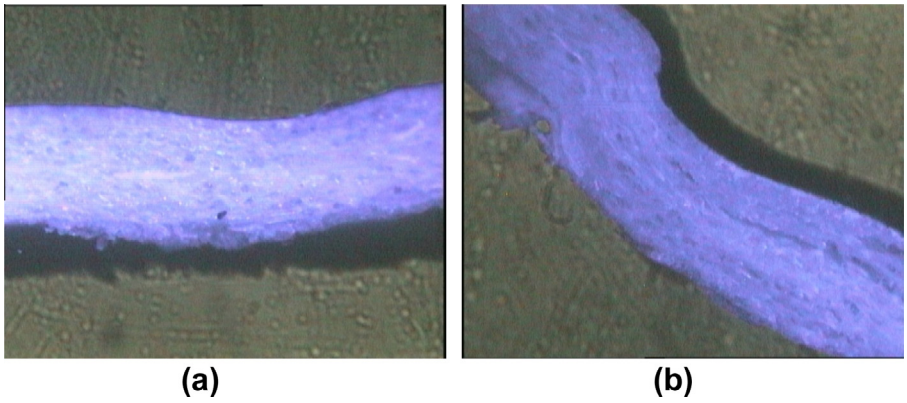

Fig. 2.7. Macrographs of unbent creased samples obtained from the left side (a) and the right side (b) of the same carton (*Green L1 and R2*) showing the very different indentation of nominal identical creases.

classes of simplified constitutive law, in order to grasp their very distinctive behavior:

- *Pseudo-linear loading response*. A monotone very regular trend, until the ultimate moment m_1 is attained at 180°. Applicable to a cut crease or to a heavy punched and damaged paperboard (*e.g.* crease **c**, Fig. 2.3).
- *Pseudo-elasto-plastic loading response*. After the initial linear phase, ending at θ_1 where the moment is m_1, this maximum value remains constant up to 180°. Applicable to dashed creases (**d**, Fig. 2.4).
- *S-shaped response*. The behavior is subdivided into several stages (*cf.* Fig. 2.5):
  - the initial phase is pseudo-parabolic, with a quasi-linear starting phase and a maximum moment $m_1$attained at θ_1, where the stiffness is zero;
  - then two pairs of unstable-stable branches link the (analytical) maxima and minima; the characteristic points are listed in the sequence $[(m_1,\theta_1), (m_2,\theta_2), (m_3,\theta_3), (m_4,\theta_4), (m_5,180)]$, as shown in Fig. 3.1. In each interval (θ_i,θ_j) the constitutive function is locally invertible. Applicable to normal creases (**n**) with moderate indentation (damage).
- *Monotonic unloading response*: monotone, pseudo-parabolic, very regular trend from the ultimate moment until the zero moment attained at θ_U. The possible very small negative moment for $0 < \theta < \theta_U$ is ignored. Applicable to every crease under unloading.

An effective analytical description of the constitutive law $m(\theta)$ can be obtained employing the following elementary *cubic splines*, in the appropriate interval (for the sake of simplicity, each spline is defined in the normalized interval [0,1]).

3.1. Elementary splines

The non-linear piece of the constitutive equations is built using the following elementary splines ($\xi := \frac{\theta-\theta_1}{\theta_2-\theta_1}$ is a normalized abscissa):

Starting Spline

$$S_0(\xi) := -m_1 \frac{1}{2}\xi(\xi^2 - 3), \tag{1}$$

in which the second derivative is imposed to be zero at the origin. In such a way the function is governed by the parameter m_1 alone and the initial slope is equal to 3/2 m_1.

Current Spline

$$S_1(\xi) := m_0 + 3(m_1 - m_0)\xi^2(1 - 2\xi/3), \tag{2}$$

with zero derivative at the extremes and control parameters m_0 and m_1.

Final Spline

$$S_3(\xi) := m_1 - \frac{1}{2}(m_2 - m_1)\xi^2(\xi - 3) \tag{3}$$

for which the second derivative at the right end is zero.

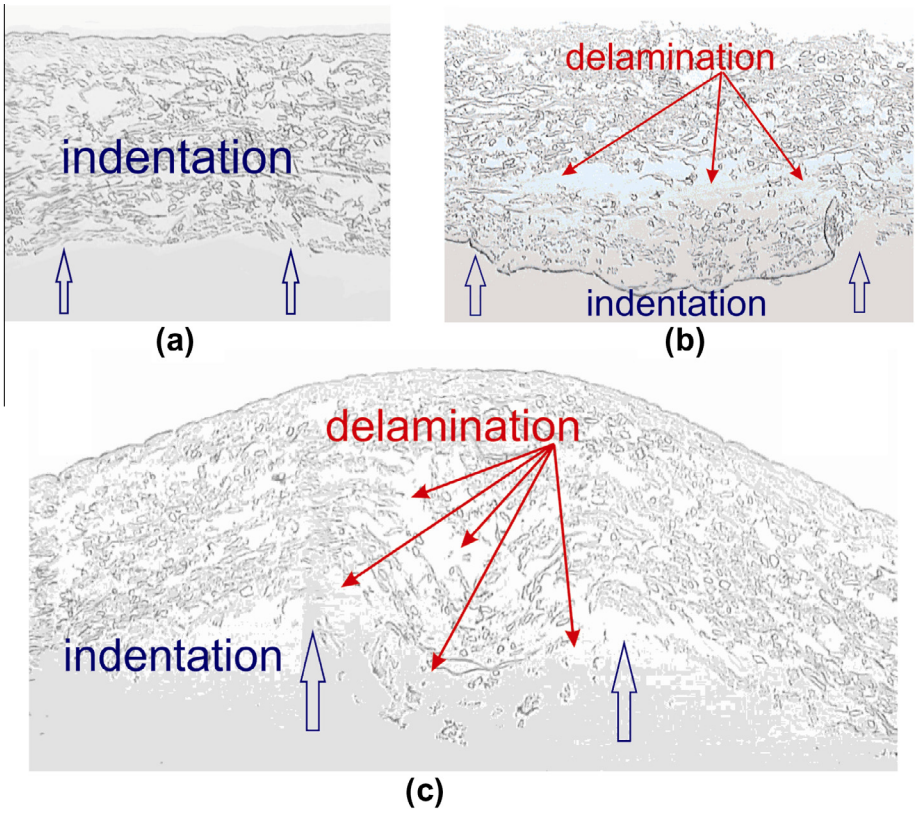

Fig. 2.8. Micrographs of histologically treated samples: (a) and (b) unbent creased paperboard with different degree of damage; (c) a sample with severe indentation, after a bending of ∼45°.

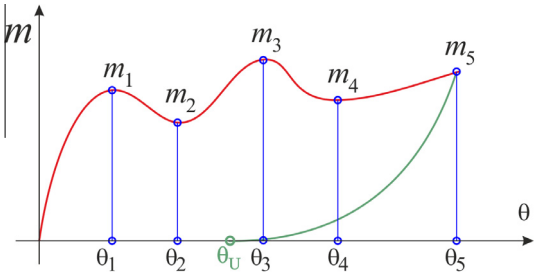

Fig. 3.1. The general constitutive equation $m_L(\theta)$: loading and unloading laws.

Unloading spline function is simply

$$S_3(\xi) := -m_2\left(\frac{\xi-\xi_1}{\xi_2-\xi_1}\right)^2\left(\frac{\xi-\xi_1}{\xi_2-\xi_1}-3\right), \tag{4}$$

similar to the previous one, with $m_1 \equiv 0$ and a rescaling of ξ.

3.2. The general constitutive equation

The general constitutive equation (for a normal crease) $m_L(\theta)$ is built as a piecewise spline. The whole range is divided in sub-intervals where the appropriate splines above defined elementary functions are employed: Starting spline (*pseudo-elasto-plastic loading*), Current splines (*S-shaped response*), Ending spline and Unloading spline, as shown in Fig. 3.1.

For the more simple behavior, the number of the intervals can be reduced accordingly.

4. Conclusion

The requirement of increasing reliability of the reconfigurable robots, manipulating origami-type cartons in packaging industry, demands an accurate characterization of mechanical behavior of the creased paperboard.

The paper presents an experimental investigation of the large bending behavior of several type of creased paperboard: *normal* (standard) crease, *continuous cut* crease and *dashed cut* crease. The response is obtained for a bending **rotation** varying **from 0° to 180°**.

The loading tests show a great variability of the mechanical behavior, which depends dramatically on the crease indentation depth, also for the specimens obtained from different sides of the same carton (a thesis supported by several micrographs).

A very interesting new result is that, when the damage induced by the crease formation is relatively small, the loading **bending response** is unusually complex: the moment function, $m_L(\theta)$, presents (up to) **two peaks** followed by **unstable branches**.

For greater indentation, the $m_L(\theta)$ is monotone.

In the unloading case, the response $m_U(\theta)$ is always monotone and is practically independent of the formation of the crease. These behaviors are described analytically using (piecewise) third degree splines.

Our tests show that the most influencing quantities (*e.g.* the crease depth) can be variable not only with time from a sample to the other, but is **significantly different within the same carton**. These results suggest that the theoretical predictive models could be not sufficiently reliable, owing to the non-controllability of the variables influencing the mechanical response.

In a companion paper, a general finite rotation kinematics and an efficient static analysis is formulated for a paradigmatic example of carton corner with 5 creases, using the constitutive relationship exhibiting unstable branches and unloading.

Acknowledgments

The first authors is personal indebted with technicians and physicians of both the Laboratory of Anatomical Pathology and Laboratory of Hematology of the Università Politecnica delle Marche, for their aid in the preparation and examination of so unusual histological specimens.

References

Allaoui, S., Aboura, Z., Benzeggagh, M.L., 2009. Phenomena governing uni-axial tensile behaviour of paperboard and corrugated cardboard. Composite Structures 87, 80–92.

Barbier, C., Larsson, P.-L., Östlund, S., 2005. On dynamic effects at folding of coated papers. Composite Structures 67, 395–402.

Beex, L.A.A., Peerlings, R.H.J., 2009. An experimental and computational study of laminated paperboard creasing and folding. International Journal of Solids and Structures 46, 4192–4207.

Cannella, F., Dai, J.S., 2009. Origami-carton tuck–in with a reconfigurable linkage. In: ASME/IFToMM International Conference on Reconfigurable Mechanisms and Robots (ReMAR 2009), London.

Cannella, F., Dai, J.S., Clari, D., 2012. Automatic folding of cartons using a reconfigurable robotic system. In: Second ASME/IEEE International Conference on Reconfigurable Mechanisms and Robots (ReMAR 2012), Tianjin, China.

Cannella, F, Pupilli, M., Mentrasti, L., D'Imperio, M., Dai, J.S., 2013. Mechanical properties of carton creases, under submission.

Carlsson, L., De Ruvo, A., Fellers, C., 1983. Bending of creased zones of paperboard related to interlaminar defect. Journal of Material Science 18, 1365–1373.

Dai, J.S., Rees Jones, J., 1999. Mobility in metamorphic mechanisms of foldable/erectable kinds. Journal of Mechanical Design ASME 121 (3), 375–382.

Dubey, V.N., Dai, J.S., 2006. A packaging robot for complex cartons. Industrial Robot 33 (2), 82–87.

Giampieri, A., Perego, U., Borsari, R., 2011. A constitutive model for the mechanical response of the folding of creased paperboard. International Journal of Solids and Structures 48, 2275–2287.

Hicks, B.J., Mullineux, C.B., McPherson, C.J., Medland, A.J., 2004. An energy-based approach for modeling the behavior of a packaging material during processing. Proceedings of the Institution of Mechanical Engineers, Part C: Journal of Mechanical Engineering Science 218, 105–118.

Mentrasti, L., Cannella, F., Pupilli, M., Dai, S.J., 2013. Large bending behavior of creased paperboard. II: Structural analysis. International Journal of Solids and Structures, under submission.

Mullineux, G., Matthews, J., 2010. Constraint-based simulation of carton folding operations. Computer-Aided Design 42, 257–265.

Nagasawa, S., Fukuzawa, Y., Yamaguchi, T., Tsukatani, S., Katayama, I., 2003. Effect of crease depth and crease deviation on folding deformation characteristics of coated paperboard. Journal of Materials Processing Technology 140, 157–162.

Nygårds, M., Just, M., Tryding, J., 2009. Experimental and numerical studies of creasing of paperboard. International Journal of Solids and Structures 46, 2493–2505.

Ostoja-Starzewski, M., Stahl, D.C., 2000. Random fiber networks and special elastic orthotropy of paper. Journal of Elasticity 60, 131–149.

Ramasubramanian, M.K., Wang, Y., 2007. A computational micromechanics constitutive model for the unloading behavior of paper. International Journal of Solids and Structures 44, 7615–7632.

Sato, J., Hutchings, I.M., Woodhouse, J., 2008. Determination of the dynamic elastic properties of paper and paperboard from the low-frequency vibration modes of rectangular plates. APPITA Journal 61 (4), 291–296.

Suhling, J.C., Rowlands, R.E., Johnson, M.W., Gunderson, D.E., 1985. Tensorial strength analysis of paperboard. Experimental Mechanics 25 (1), 75–84.

Vannucci, P., 2010. On special orthotropy of paper. Journal of Elasticity 99, 75–83.

Yao, W., Dai, J.S., 2008. Dexterous manipulation of origami cartons with robotic fingers based on the interactive configuration space. Journal of Mechanical Design 130 (2), 022303:1–022303:8.